

High-pressure phase transitions and equation of state of the III-V compound InAs up to 27 GPa

Yogesh K. Vohra, Samuel T. Weir, and Arthur L. Ruoff

Department of Materials Science and Engineering, Cornell University, Ithaca, New York 14853

(Received 4 February 1985)

The III-V semiconductor compound InAs has been studied under high pressure in a diamond-anvil cell up to 27 GPa by energy-dispersive x-ray diffraction using the Cornell High Energy Synchrotron Source (CHESS). It shows the zinc-blende-to-rocksalt transformation at (7 ± 0.2) GPa and a further transformation at (17 ± 0.4) GPa to a β -Sn-type structure with increasing pressure. The zinc-blende-to-rocksalt phase transition which is associated with metallization is accompanied by a 17% volume collapse while the rocksalt to the β -Sn transformation has no volume discontinuity within experimental errors. This structural sequence is the same as that observed in several II-VI compounds under high pressures. The results are discussed in view of theoretical pseudopotential total-energy calculations of III-V compounds in various phases and comparison is made with available experimental data on InP and InSb.

INTRODUCTION

The group-IV semiconductors Si and Ge, III-V zinc-blende semiconductor compounds, and II-VI compounds have been studied extensively under high pressures for metallization and the associated structural phase transitions. The early melting,^{1,2} resistivity,³ and structural studies^{4,5} have recently been complemented by Raman scattering studies^{6,7} under high pressures. From high-pressure resistivity measurements, the pressure-induced phase transition to the metallic state in InAs was first reported at 8.46 GPa by Minomura and Drickamer.³ In a high-pressure x-ray-diffraction study Jamieson⁴ reported a phase transition from the zinc-blende to rocksalt phase at $V/V_0 = 0.926$ with a volume collapse of 18.8%, although no quantitative relative intensity measurements were made. Subsequent resistivity measurements by Pitt and Vyas⁸ reported the transition at (6.9 ± 0.2) GPa. In the Raman scattering studies on semiconductor-grade single-crystal InAs under hydrostatic pressures by Jayaraman *et al.*,⁷ the phonons were seen at 7 GPa but the Raman signal disappeared abruptly at metallization at 7.15 GPa. We have extended the high-pressure studies on InAs to 27 GPa.

EXPERIMENTAL TECHNIQUES

The InAs was studied in a diamond-anvil cell by the energy-dispersive x-ray-diffraction (EDXD) technique using the Cornell High Energy Synchrotron Source (CHESS). For details of the experimental technique, see Baublitz, Arnold, and Ruoff.⁹ The instrumentation at CHESS was further improved to incorporate automatic loading of the high-pressure cell where the pressure of the diamond-anvil cell could be changed *in situ* by remote control. This cuts down considerably the time for adjustment of the slits and allows for faster data collection. A new turntable was also used for precise rotation of the detector for changing the diffraction angle by $\pm 1^\circ$. Sodi-

um chloride was used as a pressure marker. A mixture of powdered InAs (99.999% purity)—50 wt. % NaCl (99.5% purity) was ground to ensure homogenization. The Debye-Sherrer x-ray pattern of this mixture at room pressure showed a good powder pattern with the correct proportion of sample and marker diffraction-line intensities. The sample was placed in the 150- μ m-diam hole of a stainless-steel gasket preindented to 95 μ m and placed between diamond flats of diameter 640 μ m. The NaCl marker itself acts as pressure medium. To avoid interference from the diffraction lines of the marker and to obtain good diffraction data for the high-pressure phases, one high-pressure experiment was also performed with only the InAs sample (no marker materials) and with ruby as a pressure sensor and methanol as the pressure medium.

The pressure was calculated from the measured volume of the B1 phase of NaCl using the isotherm calculated by Decker *et al.*¹⁰ and represented by the following second-order Birch equation:¹¹

$$P(\text{GPa}) = 70.905f(1+2f)^{5/2}(1+1.376f-0.868f^2), \quad (1)$$

where

$$f = \frac{(V_0/V)^{2/3} - 1}{2}, \quad (2)$$

with $B_0 = 23.635$ GPa, $B'_0 = 4.918$, and $B''_0 = -0.25$ GPa⁻¹. This equation of state has its limitations as an assumed pressure scale. (For a more complete discussion of NaCl as a primary pressure gauge, see Ruoff and Chhabildas.¹²)

RESULTS

Figure 1 shows the EDXD pattern of the InAs sample and NaCl marker mixture at room pressure (diffraction angle $\theta = 8.239^\circ \pm 0.002$). The (200), (220), (420), and (422) reflections were observed from NaCl; the (220), (331), and

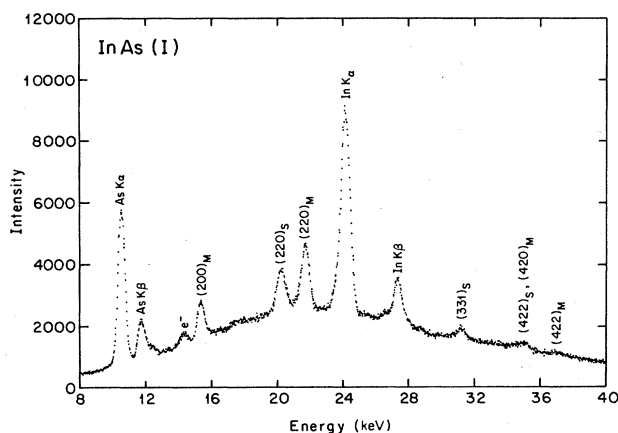


FIG. 1. EDXD pattern for the InAs-NaCl mixture at atmospheric pressure. The subscript *S* on *hkl* indices stands for the InAs sample and *M* stands for the NaCl marker. InAs is in the cubic zinc-blende phase [InAs (I), diffraction angle θ is $8.239^\circ \pm 0.002^\circ$]. The strong (311)_S line is under the In *K* α fluorescence line. The peak *e*⁻ is an escape peak. Cornell Electron Storage Ring (CESR) conditions: 4.73 GeV beam energy, 20 mA beam current.

(422) reflections were observed from the zinc-blende phase of InAs [InAs (I)]. At 7 GPa, a phase transition was observed in InAs. Figure 2 shows the EDXD patterns of an InAs-NaCl mixture at 8.46 GPa. InAs is in the rocksalt phase [InAs (II)], as is evident from the strong (200) and (220) reflections from the sample. In Table I we compare the theoretical and experimental interplanar spacings and intensities for the rocksalt phase of InAs. Upon further compression, at 16.9 GPa upon loading, another phase was seen in the InAs sample as the (200) reflection of the rocksalt phase decreases in intensity as compared to the fluorescence line and splits into the (200) and (101) peaks of a tetragonal phase (β -Sn type). Figure 3 shows the EDXD pattern for this phase at 22.4 GPa [InAs (III)]. The (220) peak from the sample also splits into the (220) and (211) peaks at the II-III phase transition, but is obscured by the In *K* α fluorescence peak and the (220) peak from the marker material. To confirm the crystal struc-

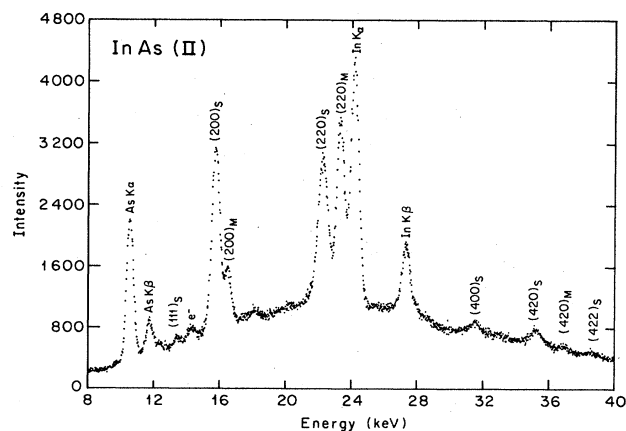


FIG. 2. EDXD pattern for InAs-NaCl mixture at 8.46 GPa. InAs is the cubic rocksalt phase [InAs (II)].

TABLE I. Comparison of calculated (Calc.) and observed (Obs.) interplanar spacings, and intensities of various diffraction lines of the rocksalt phase of InAs. $P=8.46$ GPa and $a=5.5005$ Å. The optimum sample thickness for the good fit to intensities is found to be 50 μm .

<i>hkl</i>	d_{obs} (Å)	d_{calc} (Å)	Calc. I/I_{220}	Obs. I/I_{220}
200	2.751	2.750	93	94
220	1.944	1.945	100	100
222	a	1.445	27	a
400	1.370	1.375	5	5
420	1.227	1.230	13	8
422	1.121	1.123	8	1

^aThis peak is obscured by the In *K* β fluorescence peak.

ture of phase III, one additional high-pressure run was made without any marker material, with ruby as a pressure sensor and methanol as a pressure medium. The diffraction angle was also changed to move the (220) diffraction peak of the rocksalt phase of InAs away from fluorescence peak. The splitting of the (220) diffraction line was confirmed. Table II contains a comparison of the theoretical and experimental intensities for InAs (III) obtained in this run at a pressure of 21.6 GPa, as measured by the ruby-fluorescence technique.¹³ No primitive hexagonal cell was found to fit the data on InAs (III) and account for splittings in both the (200) and (220) diffraction lines of the rocksalt phase. From the present diffraction data it is not possible to ascertain whether InAs in the β -Sn phase is ordered or disordered. The two strongest peaks expected in the ordered structure which have zero intensity in the disordered structure are (110) with an intensity of 8, relative to the (211)-peak intensity of 100, and (310) with an intensity of 3. In the present experiments and angles were such that (110) was obscured by the arsenic fluorescence peaks and (310) was obscured by the In *K* α fluorescence peak.

The equation of state (EOS) of InAs in various phases is shown in Fig. 4. The zinc-blende to rocksalt phase

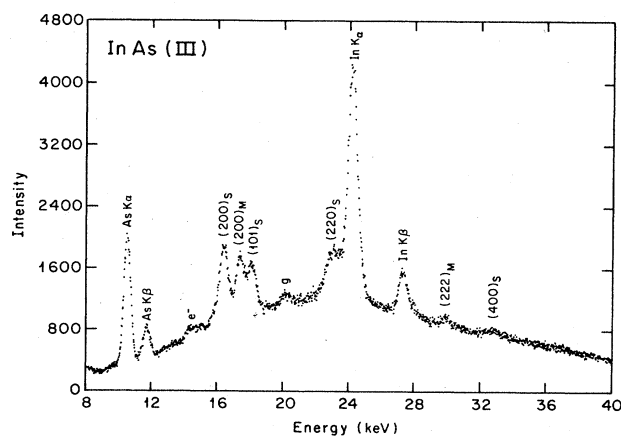


FIG. 3. EDXD pattern for the InAs-NaCl mixture at 22.4 GPa. InAs is in the tetragonal β -Sn phase [InAs (III)]. The strong (220)_M and (211)_S lines are under the In *K* α fluorescence line. The peak *g* is a gasket peak.

TABLE II. Comparison of calculated (Calc.) and observed (Obs.) interplanar spacings and intensities of various diffraction lines of the β -Sn phase of InAs. $P=21.6$ GPa, $a=5.226$ Å, and $c=2.730$ Å; the optimum sample thickness is $35 \mu\text{m}$ (diffraction angle is 8.753°). CESR conditions: 5.25 GeV and 40 mA beam current. The theoretical calculations are based on random occupation of $4a$ sites of space group $I4_1/amd$ by In and As atoms.

hkl	d_{obs} (Å)	d_{calc} (Å)	Calc. I/I_{211}	Obs. I/I_{211}
200	2.613	2.613	53	32
101	2.420	2.420	57	32
220	1.860	1.848	53	64
211	1.776	1.775	100	100
301	a	1.468	35	a
400		1.306	10	
112	1.304	1.282	20	9
321		1.280	20	
420	1.158	1.168	16	18
411		1.150	16	

^aThis peak is obscured by the In $K\beta$ fluorescence peak. present on the shoulder of the fluorescence peak.

transition (I-II) is accompanied by a $(17.0 \pm 0.2)\%$ volume collapse and the InAs (II) phase is metallic, as is known from resistivity work.^{3,8} However, at the rocksalt to the β -Sn-type phase transition, there is no measurable discontinuity in volume. The solid curve in Fig. 4 represents the fit of the data to an equation having the form of the first-order Birch equation,

$$P = \frac{3}{2} \{ a [x^{7/3} - x^{5/3}] [1 + \frac{3}{4} (b-4)(x^{2/3} - 1)] \}, \quad (3)$$

where

$$x = V_0/V,$$

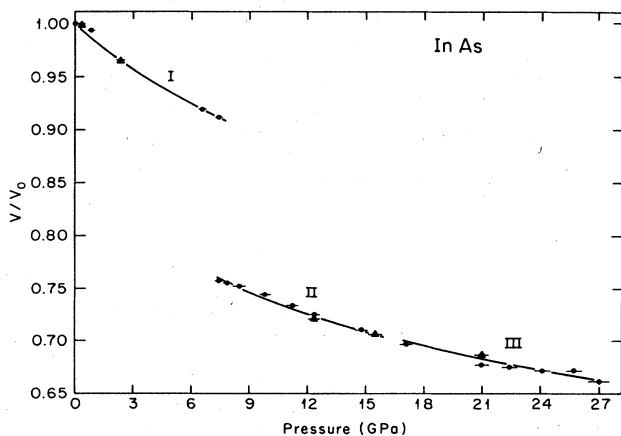


FIG. 4. Measured equation of state at room temperature for various phases of InAs. The solid circles are the loading data and the solid triangles are the unloading data. The solid curve for each phase is the first-order Birch fit to the data. The typical standard deviation for fractional volume is ± 0.003 . The bars on the pressure give the random pressure errors (1σ).

TABLE III. Results of the first-order Birch fit to the equation of state of various phases of InAs. The last column gives the extrapolated zero-pressure volumes for different phases measured relative to zinc-blende phase.

Phase	Pressure range (GPa)	a^a	b^a	$(V/V_0)_{P=0}$
InAs I	0-7	59.2 ± 5^b	6.8 ± 2	1.0
InAs II	7-15	40.6 ± 3	7.3 ± 1	0.86 ± 0.01
InAs III	17-27	46.7 ± 14	8.6 ± 3	0.83 ± 0.08

^aIf Eq. (3) exactly describes the $P(V)$ behavior and the pressure scale is exact, then $a = B_0$ and $b = B'_0$.

^bThe bulk modulus for InAs I from ultrasonic data is 58 GPa (Ref. 29).

and a and b are fitting parameters. If an equation of this form exactly describes the $P(V)$ behavior and the pressure scale is exact, then $a = B_0$ and $b = B'_0$, where B_0 is the bulk modulus at zero pressure and B'_0 is the pressure derivative of the bulk modulus at zero pressure. The fitted parameters for various phases are listed in Table III. Figure 5 shows the variation in c/a of the tetragonal phase of InAs. It is interesting to note that c/a increases with increasing pressure and becomes greater than the ideal c/a value of 0.516 above 25 GPa. The tetragonal phase of InAs was found to be stable up to the highest pressure, 27 GPa.

DISCUSSION

The present experimental work on InAs is the first observation of zinc-blende \rightarrow rocksalt \rightarrow β -Sn structural sequence under high pressure in a III-V compound. This sequence, however, is now well established in some II-VI compounds, such as CdTe,¹⁴ HgTe,¹⁵⁻¹⁷ HgSe,^{16,18} and ZnTe,¹⁹ and is expected to occur in several other compounds under high pressures. In the case of mercury chalcogenides [HgTe, HgSe, and HgS (Refs. 15 and 20)] there is, in addition, a cinnabar structure which occurs between the zinc-blende and rocksalt structures. First-principles total-energy calculations based on pseudopotentials have been done for some III-V semiconductors in

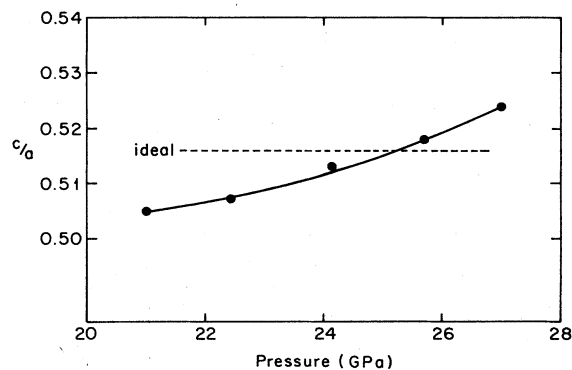


FIG. 5. Axial ratio (c/a) for the β -Sn phase of InAs as a function of pressure. The ideal c/a value of the six-coordinated β -Sn phase is also indicated.

various phases.^{21,22} Four crystal structures were examined in the theoretical work (zinc-blende, rocksalt, NiAs type, and β -Sn) for GaAs, GaP, AlAs, and AlP.²¹ Such calculations for the high-Z In-compounds (InP, InAs, and InSb) were not done because of relativistic corrections to the total energy. These crystal-structure stability calculations showed two different types of behavior as determined by cations. For the Ga compounds the β -Sn, rocksalt, and NiAs-type structures were all found to be very close in energy and are competing high-pressure structures. However, for the Al compounds, the rocksalt and NiAs-type structures are certainly favored over β -Sn-type structure. The theoretical calculations on In compounds²² indicate the zinc-blende \rightarrow rocksalt \rightarrow β -Sn structural sequence with increasing pressures for InAs and InP, but for InSb the energy difference between rocksalt and β -Sn structures is very small ($\sim 10^{-5}$ Ry).

The sequence of phase transitions observed in InAs with increasing pressure is consistent with the theoretical calculations of Ref. 22. However, the experimental transition pressures are lower; I \rightarrow II occurs at 7 GPa (theoretical estimate 11–15 GPa) and II \rightarrow III occurs at 17 GPa (theoretical estimate 50 GPa). InP undergoes the first phase transition at 10 GPa,⁶ presumably to the rocksalt structure, and we expect it to show a second transition to the β -Sn-type structure around 20 GPa or so. InSb has been studied extensively under high pressures and high temperatures and its phase diagram has been reasonably well determined up to 10 GPa and 400°C by Banus and Lavine²³ and by Yu and Spain.²⁴ The rocksalt phase does not occur in the equilibrium phase diagram of InSb; the zinc-blende phase transforms either to the β -Sn phase (InSb II) or to an orthorhombic distortion of β -Sn (InSb IV), depending on temperature. However, in amorphous InSb the pressure-induced crystallization to the metastable rocksalt phase has been seen at pressures from 0.4 to 2.8 GPa.²⁵ This indicates that the rocksalt and β -Sn phases are close in energy for InSb. Above 2.8 GPa the metastable rocksalt form transforms to β -Sn-type

structures, in close analogy to InAs. In a different experiment on sputtered rocksalt-type InSb in a cubic-anvil-type, high-pressure apparatus,²⁶ the rocksalt phase of InSb was found to be stable up to 8 GPa. The present experiment on InAs then demonstrates the basic structure sequence in indium compounds to be cubic zinc-blende \rightarrow rocksalt \rightarrow β -Sn type. The situation, however, appears to be somewhat complex in Ga compounds²⁷ and Al compounds,²⁸ and more experimentation may be needed before clear-cut crystal-structure systematics under high pressure emerge.

CONCLUSIONS

We conclude the following.

(1) The cubic zinc-blende phase, InAs, transforms to the rocksalt phase [InAs (II)] at 7 GPa. The comparison of theoretical and experimental relative intensities (Table I) confirms the previous assignment⁴ of the space group *Fm* 3*m* to phase II of InAs.

(2) A further phase transformation to phase III was found at 17 GPa with increasing pressure. The β -Sn structure has been assigned to the phase and is supported by the good fit to the interplanar spacings and relative intensities (Table II). Experiments would have to be performed at a smaller angle than used to find the extra reflections which would be present for an ordered arrangement of atoms.

(3) Within experimental capabilities, the II-III transition has no associated volume discontinuity.

(4) The equations of state are given to 27 GPa.

ACKNOWLEDGMENTS

We would like to acknowledge the support of the National Science Foundation (NSF) through Grant No. DMR-83-05798, and the Cornell Materials Science Center (supported by the NSF) for the use of their central facilities. We would like to thank the CHESS staff members for their help and Professor W. Bassett for the loan of his multichannel analyzer and detector.

¹A. Jayaraman, W. Klement, Jr., and G. C. Kennedy, *Phys. Rev.* **130**, 540 (1963).

²A. Jayaraman, W. Klement, Jr., and G. C. Kennedy, *Phys. Rev.* **130**, 2277 (1963).

³S. Minomura and H. G. Drickamer, *J. Phys. Chem. Solids* **23**, 451 (1962).

⁴J. C. Jamieson, *Science* **139**, 762 (1963).

⁵J. C. Jamieson, *Science* **139**, 845 (1963).

⁶R. Trommer, H. Muller, M. Cardona, and P. Vogl, *Phys. Rev. B* **21**, 4869 (1980).

⁷A. Jayaraman, V. Swaminathan, and B. Batlogg (unpublished).

⁸G. D. Pitt and M. K. R. Vyas, *J. Phys. C* **6**, 274 (1973).

⁹M. Baublitz, Jr., V. Arnold, and A. L. Ruoff, *Rev. Sci. Instrum.* **52**, 1616 (1981).

¹⁰D. L. Decker, W. A. Bassett, L. Merrill, and H. T. Hall, *J.*

Phys. Chem. Ref. Data **1**, 773 (1972).

¹¹F. Birch, *J. Geophys. Res.* **83**, 1257 (1978).

¹²A. L. Ruoff and L. C. Chhabildas, *J. Appl. Phys.* **47**, 4867 (1976).

¹³G. J. Piermarini, S. Block, J. D. Barnett, and R. A. Forman, *J. Appl. Phys.* **46**, 2774 (1975).

¹⁴I. Y. Borg and D. K. Smith, Jr., *J. Phys. Chem. Solids* **28**, 49 (1967).

¹⁵A. Werner, H. D. Hochheimer, K. Strossner, and A. Jayaraman, *Phys. Rev. B* **28**, 3330 (1983).

¹⁶T. L. Huang, Ph.D. thesis, Cornell University, 1984.

¹⁷T. L. Huang and A. L. Ruoff, in *Proceedings of the IXth AIRAPT International High Pressure Conference* (Albany, NY, 1983) [*Mater. Res. Soc. Symp. Proc.* **22**, Pt. III, 37 (1984)].

- ¹⁸T. L. Huang and A. L. Ruoff, *Phys. Rev. B* **27**, 7811 (1983).
- ¹⁹A. Ohtani, M. Motobayashi, and A. Onodera, *Phys. Lett.* **75A**, 435 (1980).
- ²⁰T. L. Huang and A. L. Ruoff, *J. Appl. Phys.* **54**, 5459 (1983).
- ²¹S. Froyen and M. L. Cohen, *Phys. Rev. B* **28**, 3258 (1983).
- ²²T. Soma, *J. Phys. C* **11**, 2681 (1978).
- ²³M. D. Banus and M. C. Lavine, *J. App. Phys.* **40**, 409 (1969).
- ²⁴S. C. Yu and I. L. Spain, *J. Appl. Phys.* **49**, 4741 (1978).
- ²⁵K. Asaumi, O. Shimomura, and S. Minomura, *J. Phys. Soc. Jpn.* **41**, 1630 (1976).
- ²⁶M. Asaumi and S. Minomura, *J. Phys. Soc. Jpn.* **46**, 1039 (1979).
- ²⁷M. Baublitz, Jr. and A. L. Ruoff, *J. Appl. Phys.* **53**, 6179 (1982).
- ²⁸M. Baublitz, Jr. and A. L. Ruoff, *J. Appl. Phys.* **54**, 2109 (1983).
- ²⁹K. Kunc, *Ann. Phys. (Leipzig)* **8**, 319 (1973).